

Haploinsufficiency, rather than the effect of an excessive production of soluble CD95 (CD95 Δ TM), is the basis for ALPS Ia in a family with duplicated 3' splice site AG in *CD95* intron 5 on one allele

Joachim Roesler, Jose-Maria Izquierdo, Martin Ryser, Angela Rösen-Wolff, Manfred Gahr, Juan Valcarcel, Michael J. Lenardo, and Lixin Zheng

Autoimmune lymphoproliferative syndrome type Ia (ALPS Ia) is caused by mutations in the *CD95/APO1/FAS (TNFRSF6)* gene, which lead to a defective CD95 ligand (CD95L)-induced apoptosis. Soluble CD95 (sCD95) has been suggested to play an important role in the pathogenesis of diverse autoimmune and malignant diseases by antagonizing CD95L. Here we evaluate a family with 4 of its 5 members harboring an ex-6-3C→G mutation that affects the splice cis regulatory region (cctacag/ex-6→cctagag/ex-6) of the *CD95* gene. The mutation

causes skipping of exon-6, which encodes the transmembrane region of CD95, and thereby leads to an excessive production of sCD95 in all 4 affected individuals. The mutation is associated with a low penetrance of disease phenotype and caused mild and transient ALPS in one male patient whereas all other family members are completely healthy. In all family members with the mutation we found that the cell surface expression of CD95 was low and the activated T cells were resistant to CD95-induced apoptosis. Unexpectedly, excessive production

or addition of sCD95 had no effect on the CD95-induced apoptosis in diverse cells. In contrast, increasing the surface expression of CD95 was able to correct the defect in apoptosis. Thus we conclude that the ALPS in the one male patient was caused by haploinsufficiency of membrane CD95 expression. Our data challenge the hypothesis that sCD95 causes autoimmunity. (Blood. 2005;106:1652-1659)

© 2005 by The American Society of Hematology

Introduction

CD95 (Fas, Apo1, TNFRSF6) is a transmembrane receptor belonging to the tumor necrosis factor superfamily.¹ Upon CD95 ligand (CD95L) stimulation, CD95 can induce programmed cell death (also referred to as apoptosis). Apoptosis is crucial for homeostasis of the immune system.²⁻⁴ It can down-regulate an immune response after the elimination of antigens; it is also involved in removing autoreactive or futile cells and in extinguishing malignant lymphatic cells or their genetically altered precursors.^{5,6} Recently, defects in genes regulating apoptosis have been discovered causing the clinical picture of autoimmune lymphoproliferative syndrome (ALPS),⁷⁻⁹ or an ALPS-like clinical manifestation.¹⁰ ALPS (also called Canale-Smith syndrome^{6,10-12}) is characterized by recurrent or more often chronic, benign, sometime massive lymphadenopathy; splenomegaly of early onset; autoimmune phenomena such as thrombocytopenia or hemolytic anemia; and less frequently, malignant lymphoma.^{5,6} In addition, CD4/CD8 double-negative, α/β receptor-positive T cells are often present. Further immunophenotypic characteristics have been detailed previously.¹³ However, even within one family, members who carry the same genetic defect can have diverse clinical phenotypes, including mild, reversible symptoms if any, severe autoimmune phenomena, and/or different malignancies.⁵ Furthermore, many patients come up with improvement of their symptoms when they grow older. According to the Online Mendelian Inheritance in Man (OMIM) nomenclature,

several types of ALPS exist.^{7,9,12,14-20} ALPS Ia, the most common form, is associated with mutations in the *CD95* gene, in ALPS Ib the *CD95L* gene is affected, whereas mutations in the *CASP10* gene lead to ALPS II, and cases without defined mutations are termed ALPS III. Other authors refer to the latter form as ALPS-like disease (ALD).¹⁰ ALPS induced by somatic mutations has also been described.²¹

The majority of ALPS Ia cases is due to mutations in the death domains of the *CD95* gene. The penetrance of its phenotypes is high because the mutant proteins exert dominant-negative effects on function of the wild-type CD95 protein. In contrast, there are forms of ALPS Ia with low penetrance, which have been shown to be due to haploinsufficiency. In this case, *CD95* gene mutations prevent the affected alleles from expressing a normal amount of functional CD95 proteins.²²

Pro- and antiapoptotic stimuli must be balanced carefully in the immune system in order to achieve effective homeostasis without causing "collateral tissue damage." Alternative splicing plays a critical role in regulation of apoptosis under many circumstances.²³⁻²⁸ It has previously been strongly suggested that soluble CD95 (sCD95), a translational product of alternatively spliced isoforms of CD95 mRNA that lacks exon-6, can block apoptosis through CD95.²⁹⁻³⁴ *CD95* exon-6 encodes the transmembrane domain and is therefore needed for cellular expression of the

From the Department of Pediatrics, University Clinic Carl Gustav Carus, Dresden, Germany; the Centre de Regulacio Genomica, Barcelona, Spain; and the Laboratory of Immunology, National Institute of Allergy and Infectious Diseases, National Institutes of Health, Bethesda, MD.

Submitted August 16, 2004; accepted April 20, 2005. Prepublished online as *Blood* First Edition Paper, May 3, 2005; DOI 10.1182/blood-2004-08-3104.

The online version of this article contains a data supplement.

Reprints: Joachim Roesler, Department of Pediatrics, University Clinic Carl Gustav Carus, Fetscherstr 74, 01307 Dresden, Germany; e-mail: roeslerj@res.urz.tu-dresden.de.

The publication costs of this article were defrayed in part by page charge payment. Therefore, and solely to indicate this fact, this article is hereby marked "advertisement" in accordance with 18 U.S.C. section 1734.

© 2005 by The American Society of Hematology

protein. This soluble form of CD95 has been postulated to bind and thus to neutralize CD95L. At the CD95 pre-mRNA level, the inclusion of exon-6 is up-regulated by the binding of cytotoxic granule-associated RNA binding protein 1 (TIA-1) or TIA-1 related protein (TIAR) to the U-rich region in intron-5 directly downstream of exon-5 (Figure 1).³³ This process facilitates the 5' splice-site recognition and the selection of the splice partner at the 3' end of the intron-5. We here describe for the first time 4 members of a family who carry a heterozygous double "ag" in intron-5 directly upstream of exon 6. This mutation alters the 3' splice-recognition site of the intron and therefore causes a defect in splice regulation, leading to excessive production and secretion of sCD95. Unexpectedly, such excessive sCD95 serum levels can be compatible with excellent health.

Patients, materials, and methods

Informed consent for blood drawing, functional tests, and genetic analysis was obtained from the patient and his relatives. Study protocol was approved by the Ethical Commission of the Medical Faculty of the Technical University Dresden, Germany. RhsSuperCD95Ligand (super FasL; ALX-522-020-C005) was purchased from Alexis Biochemicals (Lausen, Switzerland). Recombinant human soluble CD95 (rh-sFas; cat no. 554 336) was from BD Biosciences, Pharmingen (Franklin Lakes, NJ). Immunoglobulin M (IgM)–CD95 agonistic antibody CH-11 clone was from Clontech (Palo Alto, CA). Human Apo-1/CD95 agonistic antibody (cat no. KHS9501) was from Biosource (Camarillo, CA).

Purification of genomic DNA

For isolation of DNA, the QIAamp kit (Qiagen, Hilden, Germany) was used according to the protocol provided. Briefly, 200 μ L whole blood was lysed by proteinase K, and nucleic acids were denatured by addition of ethanol (96%), absorbed to the silica membrane provided, washed, and eluted. The A_{269/280} ratio was 1.5 to 1.8, and the DNA yield was 4 μ g to 6 μ g in 200 μ L Tris, EDTA (ethylenediaminetetraacetic acid) (TE) buffer.

mRNA isolation and cDNA synthesis

For the analysis of the CD95 mRNA from peripheral mononuclear cells (PBMCs) and from Epstein Barr virus (EBV)–transformed B cells, the Dynabeads mRNA direct kit (Dyna, Oslo, Norway) and the Superscript preamplification system for first-strand cDNA synthesis (GibcoBRL, Eggenstein, Germany) were used according to the instruction manuals. Briefly, 4 \times 10⁶ cells were lysed, homogenized, and incubated with oligo (dT)₂₅ beads. Using magnetic separation, washing steps included 2x lithium dodecyl sulfate (LiDS) and 3x standard washing buffer. After elution, 20 μ L mRNA solution was incubated with oligo (dT)₁₂₋₁₈ primer, polymerase chain reaction (PCR) buffer including MgCl₂, deoxynucleoside triphosphate (dNTP) mix, dithiothreitol (DTT), and superscript II reverse transcriptase for 50 minutes at 42°C.

PCR conditions

Thermo stable DNA polymerase, "Amplitaq Gold with Gene Amp^R," and 10x buffer containing 15 mM MgCl₂ were purchased from Perkin Elmer (Weiterstadt, Germany). The buffer (10 μ L) was mixed with 5 μ L dNTPs (10 mM of each), 5 μ L of each primer (100 ng; Table 1, Figure 1), 10 μ L genomic or complementary DNA solution, 0.5 μ L polymerase (5U), and 64.5 μ L ddH₂O. The cycle program included 10 minutes at 94°C to denature the DNA, 35 cycles of 45 seconds at 94°C, 45 seconds at 60°C, 90 seconds at 72°C, and a 5-minute final extension at 72°C. The PCR products were partly cleaned and concentrated using Microcon-50 filter devices (Amicon, Witten, Germany). The retention was diluted with ddH₂O to a total volume of approximately 30 μ L, and the DNA content was determined by spectrometry (at 260 nm).

Table 1. Sequences of primers and probes

Primers	
cDNA cloning	
CF1	5' CAA GAA TTC AGG AAT CAT CAA GGA ATG CAC ACT
CR1	5' TCC TCT AGA CTG ACT CCA GCA ATA GTG GTG ATA TAT T
RT-PCR	
CF2	5' ATG TGA ACA TGG AAT CAT CAA GGA ATG
CR2	5' AGT TGA ACT TTC TGT TCT GC
TaqMan PCR	
TF1	5' ATC CAG ATC TAA CTT GGG GTG G
TR1	5' TGT GCT TTC TGC ATG TTT TCT GT
P1 (probe)	5' TTT GTC TTC TTC TTT TGC CAA TTC CAC TAA T - FAM
TF2	5' GCA CAC TCA CCA GCA ACA CC
TR2 (=TR1)	5' TGT GCT TTC TGC ATG TTT TCT GT
P2 (probe)	5' AGT GCA AAG AGG AAG TGA AGA GAA AGG AAG - FAM
Genomic	
GF1	5' GGC CCC TAA TTT ACA AAG TGC CA
GF2	5' CCA ACC CCA TGG AAA GAT GTG
GR1	5' GTT CTG AGA AGG GAA AAT TGA ATA CT
GR2	5' CGC TAA AGG CAA GGC AAA CTT

Positions are marked in Figure 1. Forty-two more primers were used for complete genome sequencing (not shown).

Real-time TaqMan PCR (quantitative PCR)

Primers and probes (Table 1, Figure 1) were designed using the primer express software provided by the manufacturer (PRISM 7700 sequence detection system, 7700 SDS; Applied Biosystems, Foster City, CA). The instruction procedures for the TaqMan EZ RT-PCR kit (Applied Biosystems) were optimized for Mn (OAC)₂, primer (20 μ L), and probe 6-carboxyfluorescein (FAM; 10 μ L) concentrations. For each experiment, 20 ng mRNA was used and GAPDH-JOE (glyceraldehyde-3-phosphate dehydrogenase as a "housekeeping" gene, GAPDH) was coamplified as an internal control. The results (ordinate, Figure 3B-C) are given as reciprocal values of the cycle threshold (CT).

Cycle sequencing

The PE/ABI BigDye terminator-cycle sequencing kit was purchased from Perkin Elmer (Weiterstadt, Germany) and was used to determine the sequence of the CD95 gene according to the provided protocol. Briefly, after mixing 1 μ L PCR product (100 ng DNA) with 1 μ L primer (100 ng), 2 μ L terminator-ready reaction mix (containing Mg²⁺, pyrophosphatase, and polymerase), and ddH₂O to a final reaction volume of 10 μ L, the following cycle conditions were applied 25 times: 96°C for 10 seconds, 50°C for 5 seconds, and 60°C for 4 minutes; samples stored at 4°C forever (Trio Thermoblock; Biometra, Göttingen, Germany). The sequence was determined using a Sequagel 4.5% (National Diagnostics, Atlanta, GA) and a PE/ABI 377 automatic sequencer (Applied Biosystems). The sequences were aligned with both the standard sequence and the sequence of a healthy control using the ABI 377 sequence navigator software. Aberrant sequences were always confirmed on both DNA strands and in a second DNA sample to avoid PCR artifacts. On the genomic level, all exons of the CD95 gene including 20 bp or 30 bp of the adjacent introns and also the whole introns 5 and 6 were sequenced.

The most important primers for PCR and sequencing are given in Table 1 and Figure 1.

Flow cytometry determination of CD95 expression

PBMCs were prepared using lymphocyte separation medium (Gibco BRL) and isolated by standard gradient centrifugation techniques followed by hypotonic lysis of remaining erythrocytes. After activation with 10 μ g/mL phytohemagglutinin (PHA; Sigma L9132) for 24 hours, and different time intervals (1-5 days) of activation with 1 ng/mL IL2 (Sigma I-2644), the cells were incubated for 30 minutes on ice with 5 μ g/mL mouse IgM (Becton Dickinson, Heidelberg, Germany) isotype control or 5 μ g/mL anti-CD95

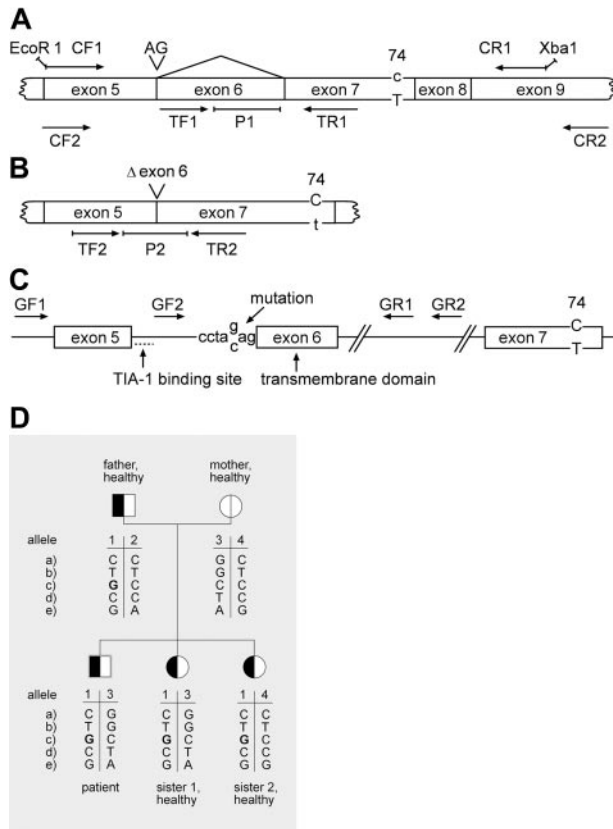


Figure 1. Positions of primers and probes in the CD95 genomic and cDNA, and overview of important sequences in the patient with ALPS. (A) cDNA, including exon 6. There is an AG insert in a few strands that is linked to a C in the polymorphic position 74 (position 74 downstream of the 5' end of exon 7, same as position 836 bp downstream of the first translated ATG). Most normally spliced cDNA (including exon 6, but not the extra AG) has a T in position 74. Primers CF1 and CR1 were used for cloning; CF2 and CR2 for RT-PCR; and TF1, P1, and TR1 for TaqMan PCR to quantify the normally spliced form. (B) Splice forms that lack exon 6 and hence the transmembrane domain. They mostly have a C in position 74. These forms were quantified by TaqMan PCR using TF2, P2, and TR2. (C) Genomic sequence with a mutation C→G in position -3 upstream of exon 6 on one allele and with the C/T polymorphism in exon 7. The primers used for genomic sequencing (GF1, GF2, GR1, GR2), the TIA-1 binding site, and the transmembrane domain are marked. (D) Pedigree and SNP haplotyping. Analysis of intronic SNPs upstream of exon 5 (a, b) and downstream of exon 7 (e), the C/T SNP expressed in exon 7 (d) 836 bp downstream of the first translated ATG (see position 74 A, B, C, also used in Table 2), and the mutation ex-6-3C→G (c), which is associated with excessive sFas production, decreased mFas expression, and apoptosis (Figures 2 and 4).

monoclonal antibody (mAb) CH-11. Antibody binding was detected with fluorescein isothiocyanate (FITC)-conjugated goat anti-mouse IgG antibody (Becton Dickinson). Lymphocytes (10 000) were measured by flow cytometry and analyzed after gating on vital cells using a FACSCalibur (Becton Dickinson).

Apoptosis measurement by flow cytometry

PBMCs were incubated in PHA and later activated with interleukin 2 (IL2) for 5 days as described in "Flow cytometry determination of CD95 expression." Apoptosis was induced by incubation of the cells with anti-CD95 mAb or soluble super CD95L for 16 hours and then determined with the annexin V-FITC kit (PN IM3546; Immunotech, Marseille, France). This assay indicates an early phase of apoptosis by FITC-annexin binding to phosphatidyl serine, which turns to the outer cell membrane surface (green fluorescence), whereas cell death can be measured by propidium iodide, which stains the DNA of cells that lost their membrane integrity (red fluorescence). As agonistic antibodies, the CH-11 IgM clone was used for diagnosis and when effectiveness in inducing apoptosis was

essential, whereas the Apo-1 antibody (ALEXIS Biochemicals Products) was used for graded responses.

Determination of the sCD95 secretion

PBMCs were incubated with PHA and activated with IL2 as described in "Flow cytometry determination of CD95 expression" for 0, 2, or 5 days. The medium containing IL2 was changed 48 hours before measurement and the suspension was adjusted to 10^6 cells/mL. Aliquots of 50 μ L of the cell supernatant were tested for sCD95 in appropriate dilutions using the MBL sCD95 (S) enzyme-linked immunosorbent assay (ELISA) kit (no. 5251; Medical and Biological Laboratories, Nagoya, Japan) through standard sandwich ELISA techniques. Measurements of CD95 expression, secretion of sCD95, apoptosis, and determination of the alternatively spliced forms of CD95 mRNA were also performed on optimally proliferating EBV-transformed B cells without additional stimulation.

Incubation of Jurkat cells in serum or cell supernatant containing sCD95

Cells were incubated in 70% serum or supernatant and 30% standard medium before super CD95L was added. Apoptosis was measured 20 hours later.

Plasmids and transfection

AU1-(DTYRY1)-tagged CD95-encoding plasmid (pCI-backbone) has been used before.⁸ AU1-tagged CD95-del6 (CD95 Δ TM) plasmid for sCD95 production was made by applying site-directed mutagenesis to the original CD95 plasmid using the Stratagene QuikChange XL Kit (cat no. 200 516; La Jolla, CA) according to the instructions of the manufacturer. In short, forward and reverse primers were designed comprising 12 bp of the 3' exon-5 and 12 bp of the 5' exon-7 to bridge exon-6. Methylated original CD95 plasmid derived from bacteria was used as the template and both primers were added for an 18-cycle PCR; the remaining methylated template was digested with the *DpnI* provided, and the PCR product was used to transform XL 10-Gold competent bacteria. Bacterial colonies growing under appropriate selection were selected for further processing and correct plasmids were purified using the Marligen Biosciences Maxiprep system (cat no. 11 452-026; Ijamsville, MD). The correctness of CD95-del6 was verified by sequencing.

Optimally proliferating Jurkat (ATCC, Rockville, MD) or the mouse thymoma BW cells⁸ were suspended at 10^7 cells/mL, and 0.4 ml per transfection were used in 4-mm cuvettes together with plasmids in the indicated amounts. The cells were electroporated using a BTX machine (260 V, 1050 μ F, 720 Ohm; Pittsburgh, PA), and resuspended in 6 mL fresh medium in 6-well plates and cultured for approximately 20 hours. EBV-transformed B cells were transfected using the Amaxa biosystem (Cologne, Germany) according to the B-cell transfection protocols provided by the manufacturer.

Retroviral transduction of Jurkat cells

CD95del6 (Fas Δ TM) was cloned into a bicistronic oncoretroviral transfer vector (MFG-S-internal ribosome entry site [IRES]-enhanced green fluorescent protein [eGFP]),^{35,36} which enables eGFP coexpression under a single promoter. For control transductions, a monocistronic MFGS-eGFP vector was used. 293T cells were cotransfected with 10 μ g transfer vector, 6.5 μ g gag pol packaging plasmid, and 3 μ g vesicular stomatitis virus glycoprotein (VSV-G) envelope plasmid (pMDG) in a 10-cm dish using polyethylenimine (PEI). Supernatant containing virus particles was harvested. Optimally proliferating Jurkat cells were suspended at 0.4×10^6 cells/mL, and 0.5 mL cell suspension and 0.5 mL virus supernatant were mixed in a 24-well plate. Polybrene (8 μ g/mL) was added and the plate was centrifuged at 12 000g for 20 minutes. At 96 hours after transduction, the efficiency was analyzed by flow cytometry and found to be more than 90%. sCD95 (sFas) expression of transduced Jurkat cells was analyzed by ELISA as described.

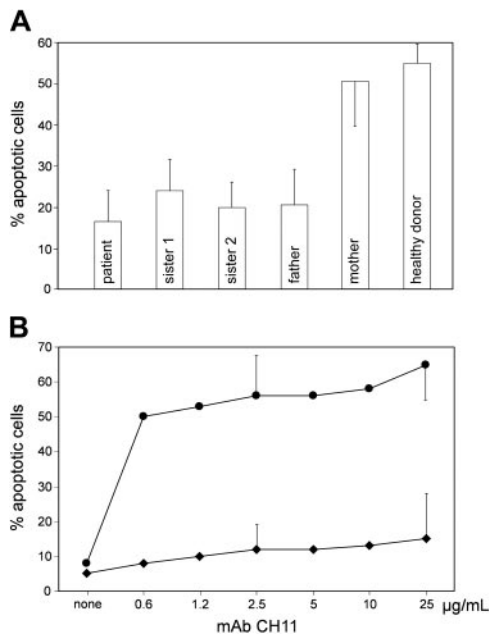


Figure 2. Apoptosis of lymphocytes from the patient and the other family members. (A) PBMCs were activated for 5 days (2 days PHA, 3 days IL2) and incubated in the absence and presence of agonistic mAb CH-11 (2.5 μg/mL) for another 24 hours. Ordinate: percent PI- and annexin-positive cells; induced minus spontaneous apoptosis is given. (B) Proliferating EBV-transformed B cells from the patient were incubated with mAb CH-11 at different concentrations. Five experiments with 2.5 μg/mL and 25 μg/mL mAb CH-11 each. Error bars indicate standard deviation. ● indicates cells from a healthy donor; ◆, cells from the patient. Induced minus spontaneous apoptosis is given. Ordinate as in A.

Coincubation assay of Jurkat and CD95L-L5178Y cells, and calculation of percent cell loss

CD95L (FasL)-expressing cells were a kind gift from Dr Sang-Mo Kang at University of California San Francisco (UCSF). These cells are a transfected mouse thymoma line expressing uncleavable human FasL on their surface and are referred to as CD95L-L5178Y cells.³⁷ L5178Y wild-type and L5178Y CD95L (FasL) overexpressing cells were coincubated with Jurkat cells that either express sCD95 (sFAS) and GFP or GFP alone. For coincubation assays all cells were suspended at 0.25 × 10⁶ cells/mL. Jurkat cell suspension (0.25 mL) was mixed with 0.75 mL L5178Y cell suspension. GFP-expressing cells were counted for 30 seconds using flow cytometry at time points 0 hours and 22 hours. Cell loss induced by CD95L (FasL)-expressing L5178Y cells was calculated as follows: 1 - [(number of vital GFP⁺ cells after a 22-hour incubation with FasL-expressing cells) / (number of GFP⁺ cells found after parallel coincubation with L5178Y wild-type cells not expressing FasL)] × 100%. The same type of calculation was used in all experiments where % cell loss is given.

Case report

The patient’s family history is unremarkable. He presented with epistaxis, thrombocytopenia (minimum 10 000/μL), splenomegaly, and cervical and axillary lymphadenopathy at age 8 years. His mother reported that the splenomegaly had already been observed shortly after birth. From age 8 to 18, the patient had thrombocytopenia that was accompanied with petechia and hematomas of the skin once or twice a year. Lymph node biopsies taken at age 10 and age 12 both showed nonspecific, chronic inflammatory lymphatic hyperplasia. The patient also presented with recurrent neutropenia (250/μL-600/μL). Antiplatelet autoantibodies were strongly positive and antineutrophil autoantibodies were weakly positive. Repeated cytologic and histologic examinations of the patient’s bone marrow revealed an enhanced granulocytopenia and normal megakaryocytes. All other findings and all routine immunologic diagnostics were unremarkable. The thrombopenia and neutropenia responded well to steroids, but autoantibodies did not.

Table 2. Phenotype of the ex-6 –3C>G mutation

	Ex6-3C→G	Normal sequence
Membrane CD95 expression*	90 ± 110	240 ± 90
sCD95 production (ng/mL)†	23 ± 7	4 ± 2
Apoptosis‡	15 ± 8	52 ± 15
Clinical phenotype	1 of 4 had transient ALPS, all 4 are healthy	Healthy control donors, n = 10

Data were presented as mean ± standard deviation; P < .01, signed rank test. *Mean channel fluorescence, arbitrary units; membrane CD95, n = 8 measurements on affected family members. †n = 8. ‡Annexin- and PI-positive activated peripheral T cells in percent (induced minus spontaneous apoptosis is given; see “Patients, materials, and methods”).

At age 12, 80% of the patient’s spleen was removed by surgery. However, it grew back to a moderately enlarged size within 3 years. Since age 18, the patient, who is now 24 years old, has had only minor lymph node swellings and no further problems. Platelet and leukocyte counts have been normal ever since. The CD4, CD8 double-negative T cells have been normal lately.

All other family members including the father are completely healthy and have never had any similar symptoms. The father and one daughter participate in sports and other physical strains along with their profession.

Results

The clinical phenotype of our patient (see “Case report”) was typical for ALPS. We found that as compared with healthy controls, the CD95-induced apoptosis was clearly reduced in the peripheral blood lymphocytes from the patient, from all family members with the respective mutation (Figure 1D, Figure 2A, and Table 2), and in EBV B cells (Figure 2B) from the patient. Because the majority of ALPS patients carry a mutation in the CD95 gene,⁶ we sequenced the patient genomic and complementary DNA for the CD95 gene. We found a C→G point mutation at position –3 of intron-5 in one allele, which led to an alteration of the splice cis regulatory region (cctacag/G→cctagag/G; Figure 1C). In accordance with this finding, sequencing of cDNA that derived from the activated PBMCs and EBV-transformed B cells revealed 3 splicing variants in the region of exons 5, 6, and 7, as diagrammed in Figure 1. Allele-specific, quantitative results were obtained by sequencing 50 individual cDNA clones from the patient. The SNP836 (position 74 in exon 7, Figure 1) clarified the maternal or paternal origin (Table 3). In the largest portion of patient cDNA, exon 6 was skipped (Figure 1B, Table 3, second column); a small portion was normally spliced and contained exon 6 (Figure 1A, Table 3, second column); and a few cDNA clones were found to contain exon 6, but had a small 2-bp insertion of AG in positions –1 and –2 upstream of this exon (Figure 1A, Table 3, fourth column). This clearly demonstrated that the additional “ag,” which was created by the mutation, was weakly active as a splice site and led to an insertion

Table 3. Different expression of the paternal and maternal CD95 allele of the patient in activated PBMCs

Allele SNP836 ex7	Δex6, n (%)	normal ex6, n (%)	insAG ex6, n (%)	Σ, n (%)
C, paternal	32 (64)	1 (2)	1 (2)	34 (68)
T, maternal	3 (6)	13 (26)	0	16 (32)
Σ	35 (70)	14 (28)	1 (2)	–

The number and percentage of the CD95 cDNA clones with the respective sequences are given. – indicates not applicable.

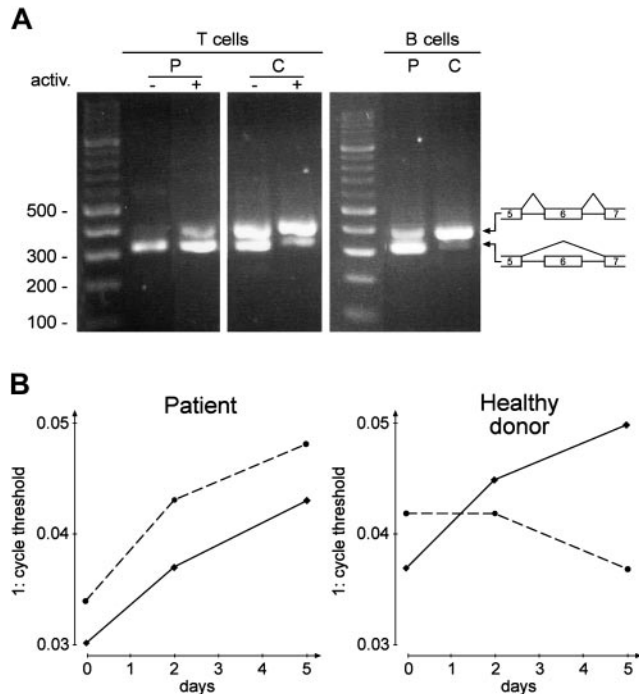


Figure 3. RT-PCR products of CD95 and CD95-del6 mRNA. (A) RT-PCR before (–) and after (+) activation (5 days as in Figure 2) of PBMCs (T cells) and of EBV-transformed B cells (B cells, $n = 5$). P, patient; C, healthy donor; primers: CF2, CR2. (B) Real-time TaqMan RT-PCR of the splice product containing exon 6 (—) and of the alternatively spliced mRNA without exon 6 (---), both from PBMCs. Primers and probes: TF1, P1, TR1; TF2, P2, TR2; abscissa: days of activation; ordinate: reciprocal cycle threshold. The same experiment was performed with EBV-transformed B cells (same result as on day 5, $n = 3$, not shown).

of the normally intron-splicing consensus sequence “ag” into the CD95 RNA transcript. Also, we completely sequenced the CD95 cDNA and genomic DNA, including all its exons with extending 20 bp to 50 bp of adjacent introns from the patient. No mutation was detected on the second allele. The ALPS-affected patient and one healthy sister shared the same second *CD95* allele from their mother, whereas the other healthy sister inherited the mother’s other allele (Figure 1D). Therefore, the maternal allele does not contribute to the patient’s ALPS, at least not critically.

We found that in healthy donor lymphocytes, the ratio of wild-type (wt) to CD95-del6 was increased after lymphocyte activation as shown in Figure 3. This confirms the previous observation that during lymphocyte activation, the splicing of complete wt-CD95 mRNA is normally upregulated.²⁹ However, we found that in the patient, the splicing variant CD95-del6 was upregulated above normal range during lymphocyte activation for both primary T and B cells, as well as in autoproducting EBV B-cell lines (Figure 3A, B cells). Our data suggest that the patient lymphocytes express an elevated amount of the alternatively spliced CD95-del6 mRNA during immune responses.

Next we investigated the impact of this variant splicing of CD95 on its cell surface expression. The full-length wt-CD95 mRNA is expressed as a membrane-bound, apoptosis-mediating receptor, which is capable of binding CD95L.³² We found that after activation, the membrane CD95 expression on the patient’s PBMCs was decreased as compared with the control cells (Figure 4C, Table 2). This observation was recapitulated in EBV cell lines derived from the patient versus 5 healthy individuals by applying the same staining to these proliferating B cells (data not shown),

and also in the other family members (Figure 1D) affected by the ex-6-3C→G mutation (Figure 4C, Table 2).

CD95-del6 mRNA splicing variants are translated to sCD95 proteins, which are secreted by lymphocytes. It has been postulated that the sCD95 can bind CD95L and thus antagonize CD95L-induced apoptosis.³² In accordance with the excessive production of CD95-del6 mRNA in the patient’s lymphocytes, an approximately 7-fold increase in sCD95 was detected in the supernatant of the patient’s cells (Figure 4A-B), and in the serum of all affected family members (Figure 4D), as compared with that of the healthy control donors. The secretion of sCD95 was upregulated during activation of the patient’s lymphocytes (Figure 4B).

Next we evaluated sCD95 at the functional level. As shown in Figure 2 (see also Figure S1; see the Supplemental Figures link at the top of the online article, at the *Blood* website), the apoptosis of activated PBMCs from the patient and the other affected family members was obviously decreased as compared with control cells when these cells were stimulated by an agonistic anti-CD95 mAb CH-11 (or by super CD95L; data not shown), even though the induction of cell death was not abolished as seen in some patients with ALPS, as previously described.^{6,22} A similar reduction of CD95-induced apoptotic response was also observed in patient EBV B cells (Figure 2B). This reduction could not be overcome by increasing the concentration of the mAb CH-11 to 25 $\mu\text{g}/\text{mL}$ (Figure 2B) or even 250 $\mu\text{g}/\text{mL}$ (data not shown). Despite the excess of agonist, the fraction of apoptotic cells did not exceed 25% (or 35%, respectively). These data indicate that the patient lymphocytes are defective in CD95-induced apoptosis.

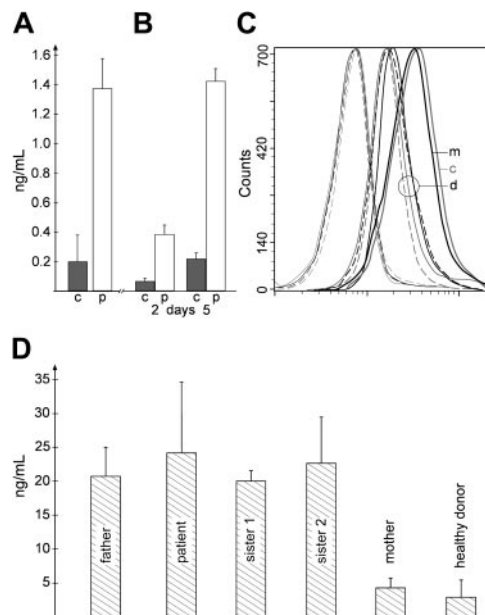


Figure 4. Secretion and serum levels of sCD95, and CD95 expression. Cell supernatant from proliferating EBV-transformed B cells (A; $n = 5$) and from PBMCs (B; $n = 2$) that were activated with PHA for 2 days and IL-2 for 3 days (5 days of total incubation) was collected to determine sCD95 secretion; p, patient; c, healthy donor. (C) CD95 expression by PBMCs after 5 days of activation; representative result, see also Table 3. In the rightmost 2 curves, m indicates mother; c, healthy control donor. For the middle group of curves, d indicates the four affected family members. The leftmost curves consist of a second antibody alone in 3 affected family members and the healthy control donor. The same result was seen in EBV-transformed B cells ($n = 5$, data not shown). (D) Serum levels of sCD95 were measured in the patient, the other family members affected by the mutation (father, sister 1, and sister 2), the healthy mother (two times in each subject), and in 6 healthy control donors. Error bars indicate standard deviation.

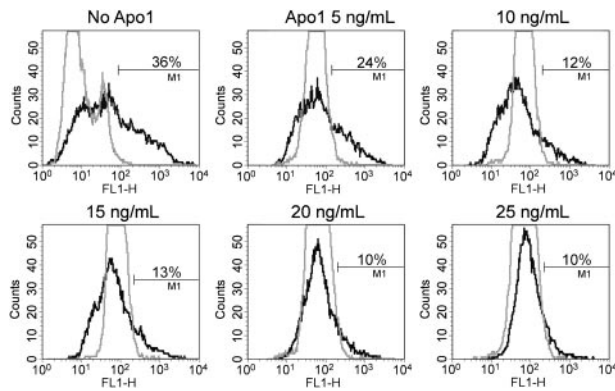


Figure 5. Functional correction of EBV-transformed B cells from the patient with ALPS. Correction was performed by transfection (Amaza system) with 20 μ g wt-CD95 AU1-tagged plasmid (black line). As negative control, patient cells were transfected with empty plasmid (gray line). The region M1 is set to contain 0.2% negative control cells. Apoptosis was induced by incubation with the agonistic mAb Apo1 for 20 hours. Percentages reflect the fraction of corrected cells that survived the mAb Apo1 challenge. AU1 staining is shown; 1 representative of 2 transfection experiments is given.

Since excessive concentrations of the multivalent anti-CD95 failed to enhance apoptosis of the patient's lymphocytes, we hypothesized that the decrease in expression of membrane-bound CD95, but not the sCD95 produced by the patient's cells, accounts for the defect of CD95-induced apoptosis. To test this hypothesis, we transfected patient EBV B cells with a plasmid that expresses an epitope-tagged (AU1) wt-CD95. As shown in Figure 5, cells supplemented with wt-CD95 (as indicated by AU1 expression) were more sensitive to anti-CD95-induced apoptosis compared with mock-transfected cells. We observed that the cells with high AU1 expression, indicating the greatest expression of CD95, were the most sensitive cells. They underwent apoptosis in response to as low as 5 ng/mL anti-CD95 stimulation. By evaluating the dose-response, we found that cells expressing modestly increased CD95 responded well to 10 ng/mL to 20 ng/mL anti-CD95 stimulation, whereas mock-transfected patient cells were resistant to much higher doses of anti-CD95 stimulation (Figure 5). Thus, the level of membrane CD95 expression is a crucial determinant of the sensitivity of lymphocytes to CD95-induced apoptosis.

Next we incubated Jurkat cells in cell-culture supernatant from patient EBV B cells or serum from the family members carrying the mutation and added agonistic antibody or CD95L. The concentrations of sCD95 in these fluids are given in Figure 4. We also incubated PKH26-labeled Jurkat cells with patient EBV B cells to test if sCD95 is effective in the microenvironment. We found no inhibition of apoptosis of Jurkat cells in any of these experiments (Figure S2). Furthermore, we observed that overexpression of sCD95 in Jurkat cells by transfection had no protective effect whether the cells were exposed to high or low levels of agonistic antibodies (Figure S3).

The mouse thymoma BW cells have been successfully used to demonstrate dominant-negative effects of mutations in the CD95 death domain.⁸ Therefore, these cells were transfected with either wt-CD95 or CD95-del6 or both (and with empty plasmid as a control, Figure 6). As shown in Figure 6C, the expression of wt-CD95 was necessary to render BW cells sensitive to apoptosis induced by specific anti-human CD95. However, the presence of human sCD95 did not interfere with the induction of apoptosis. Thus, in this coexpression model we found no inhibitory effect of sCD95.

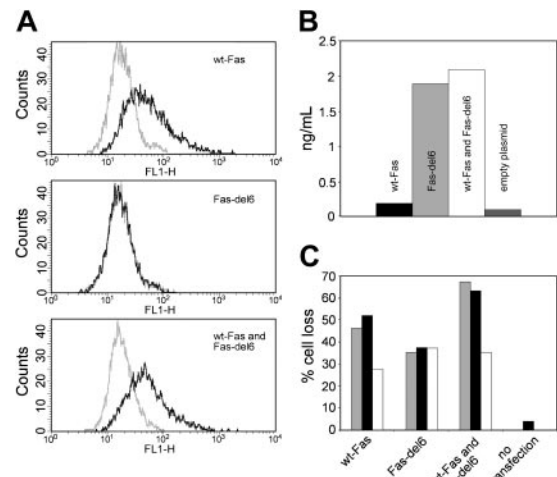


Figure 6. Production of human sCD95 did not interfere with anti-CD95-induced apoptosis in mouse BW cells. (A) Expression of human CD95 (Fas) after transfection of mouse BW cells with 20 μ g plasmids as indicated. Gray lines indicate staining with goat antimouse antibody alone; black lines, Apo1 antibody added for specific staining. (B) Secretion of human sCD95 (sFas) into the cell supernatant by BW cells 2 days after transfection. (C) Loss of transfected BW mouse cells by mAb Apo1 (□, 200 ng/mL; ■, 500 ng/mL) and Protein A or by Protein A alone (□). The average of 2 experiments is given.

To further explore the potential functions of sCD95 in apoptosis, we incubated Jurkat cells with different, at certain occasions extremely high, concentrations (10 ng/mL-1000 ng/mL) of recombinant human (rh) sCD95, and induced apoptosis of the cultured cells by super CD95L (Figure 7A). We observed only modest inhibition of apoptosis at the highest concentration of rh sCD95, and yet the inhibition was easily reversible by a moderate increase

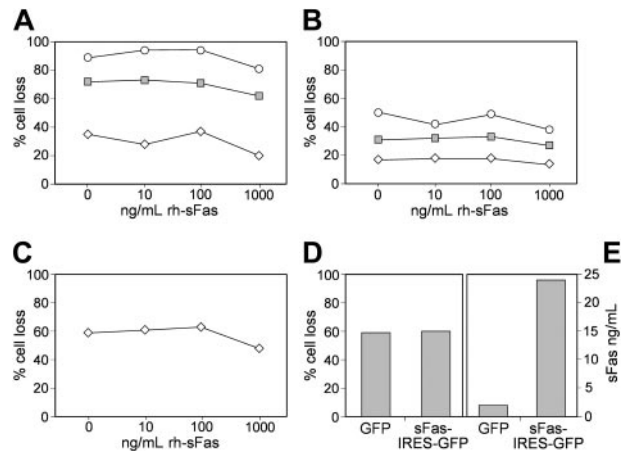


Figure 7. Insufficient inhibition of super CD95L-induced apoptosis by rh sCD95. (A) Jurkat cells and (B) normal activated peripheral T cells were incubated with rh sCD95 (rh-sFas). Abscissa: concentration of rh sCD95 (rh-sFas), ng/mL; ordinate: percent cell loss. \diamond indicates 1 ng/mL, \square , 5 ng/mL, and \circ , 25 ng/mL super CD95L (FasL) added to cell medium. $n = 2$; incubation time, 36 hours. (C) Effect of rh sCD95 (rh-sFas) on apoptosis of Jurkat target cells induced by CD95L (FasL)-expressing effector cells. Effector-target ratio, 3:1; abscissa and ordinate same as in panels A and B; $n = 6$; incubation time, 22 hours. Note: compared with the respective values at 0, 10, or 100 ng/mL, the moderate inhibition of apoptosis by 1000 ng/mL rh sCD95 (rh-sFas) is significant if all experiments (A-C) are included into the calculation (in each series cell loss is lowest when 1000 ng/mL rh sCD95 [rh-sFas] was added). $P < .016$, sign-test. (D) Apoptosis of transduced, permanently sCD95 (sFas)-secreting Jurkat target cells after incubation with CD95L (FasL)-expressing effector cells. Effector-target ratio, 3:1; ordinate same as in panel A; incubation time, 22 hours; $n = 6$. Vectors used: MFG-S-GFP, left column; MFG-S-sFas (sCD95)-IRES-GFP, right column. Cells used 1 week after transduction. (E) Respective amounts of CD95 (sFas) produced by the transduced cells in 48 hours.

in CD95L concentration. We obtained a similar result using activated peripheral T cells from healthy donors (Figure 7B). In another experiment, we induced apoptosis by effector cells expressing CD95L on their surface to evaluate if cell-to-cell contact was more sensitive to sCD95 than to apoptosis induced by soluble CD95L (Figure 7C-D). However, again only modest inhibition of apoptosis at the highest concentration of rh sCD95 was detected (Figure 7C). This minor inhibition is statistically significant if all experiments are combined (Figure 7A-C). Nevertheless, these data do not reveal a potent blocking effect for sCD95.

Finally, it remains possible that sCD95 is effective in inhibiting apoptosis in a cell-to-cell contact microenvironment if secreted by target cells. Therefore, we transduced Jurkat cells with an MFG-S-sFas (sCD95)-IRES-GFP retroviral vector (or MFG-S-GFP as a control) and checked the permanent and high sCD95 secretion one week later (Figure 7D-E). It was clearly higher than the sCD95 production by the patient's cells (Figure 4). The sCD95-secreting Jurkat target cells were identified by GFP and incubated with CD95L expressing effector cells or control cells not expressing CD95L. We found no difference in the loss of GFP-positive target cells whether or not these cells secreted sCD95 (Figure 7D).

Discussion

The most frequent form of ALPS is type Ia, which is caused by a variety of different mutations in the *CD95* gene. In the majority of cases, the mutations occur in the region encoding the intracellular death domain,^{5,7,8,22,38} and the mutant proteins exert a dominant-negative effect on CD95 signals. This can be explained as follows: transmembrane wt-CD95 associates with the mutated form (2:1 or 1:2) via the pre-ligand assembly domain³⁹ to form trimers (or bigger complexes) that are incapable of appropriately recruiting the FADD/MORT1 adaptor protein upon CD95L occupancy of the extracellular domain of CD95. Thus, the majority of the receptor trimers are defective in intracellular signaling, even if 50% of the total CD95 protein in the cell is normal. In contrast, type Ia ALPS caused mostly by extracellular mutations in *CD95* that have no dominant-negative effect^{7,14,22,39} is a result of haploinsufficiency of CD95 expression. In this case, the disease phenotype is inherited in a dominant mode with low penetrance.

We found that the lymphocytes from our patient were resistant to in vitro CD95-induced apoptosis (Figure 2) and that their level of cellular CD95 expression was decreased (Figure 4), whereas their secretion of sCD95 was elevated. However, all other family members that carry the same splice mutation seemed to be healthy albeit their high serum levels of sCD95 (Figure 4). We examined if the functional defect for CD95-induced apoptosis was caused by decreased CD95 expression, by excessive sCD95 production, or both.

Our data show that a moderate enhancement of wt-CD95 expression in patient cells by transfection could easily restore their sensitivity to CD95-induced apoptosis even in the presence of excessive sCD95 production (Figure 5). However, attempts to antagonize the sCD95 by an excess of antibody did not result in any significant change in sensitivity to apoptosis (Figure 2B). The incubation of Jurkat cells in cultures containing sCD95 from the mutant-affected family members (serum and cell supernatant) did not inhibit apoptosis, even when induced by very low amounts of CD95L. In addition, expression of sCD95 in Jurkat cells by transfection failed to reduce their sensitivity to CD95-induced

apoptosis. Thus, our data suggest that sCD95 is not potent in neutralizing CD95L for apoptosis induction.

Results using BW cells^{8,22} (Figure 6), rh sCD95, and target cells expressing sCD95 (Figure 7) further strengthen our conclusion that the soluble receptor is not a very potent regulator of cell death under any condition tested. We therefore conclude that the regulatory and pathogenic function of sCD95 may have been overestimated.^{32,34,40-43}

Our results strongly suggest that the transient ALPS of the patient in this family is caused by haploinsufficiency of membrane CD95, and that the increased sCD95 is of minor importance, if it has any effect at all, in causing the cellular resistance to CD95-induced apoptosis. The assumption of haploinsufficiency is supported by the observation of the decreased expression of wt-CD95 in the patient's cells; the reconstitution of normal CD95-mediated apoptosis by transfection of wt-CD95; the lack of significant interference on the wt-CD95 from the mutated allele; and the low penetrance in the family. As mentioned in "Introduction," this low penetrance has been previously observed in other ALPS families with haploinsufficiency.^{7,14,22,39} In accordance with these reports, we propose that a sufficient expression of full-length CD95 protein on lymphocyte membrane is crucial for keeping normal apoptosis responses to CD95 stimulation.

An important role for sCD95 has been hypothesized in malignant and autoimmune diseases.^{32,34,40-43} However, in these reports, high concentrations were often used in the analysis of in vitro and in vivo functions of sCD95, and we confirm some effect of such high concentrations (Figure 7). The impact of physiologic concentrations as measured by other investigators and us remains unclear. The biochemical mechanism by which sCD95 could antagonize the ability of CD95L in triggering membrane-CD95 receptor has not been established. Efficient ligand (CD95L) binding requires oligomerization of the receptor (sCD95) and it has not been shown that such proper oligomerization or conformation of the shed receptor is achieved.

Even though the general role of sCD95 remains inconclusive at the moment, our data do not support the hypothesis of its great importance in the pathogenesis of autoimmune diseases, and alternative assumptions should be discussed. Sensitizing leukocytes for CD95 apoptosis includes, among other regulatory steps, up-regulation of CD95 transcription and regulation of pre-mRNA splicing. The physiologic role of this splice regulation simply may be to ensure that there is no premature sensitivity to CD95-mediated apoptosis. High levels of membrane CD95 at an early phase of activation can be prevented without necessarily interfering with the CD95 function, and this can be achieved by just excluding exon 6 and thereby the membrane integration domain from the CD95 molecule. It is also likely that *CD95* transcription and splicing are regulated by different signals. If this is the case, high expression levels of CD95 will depend on the simultaneous presence of more than one proapoptotic signal.

Acknowledgments

We would like to thank Helen Su, Keiko Sakai, Jennifer Puck, and Steve Straus (NIH, Bethesda, MD) for their support and interesting and helpful discussion, and Romy Lehmann and Andrea Groß (TU Dresden, Germany) for excellent assistance and graphic design, respectively.

References

- Nagata S. Apoptosis by death factor. *Cell*. 1997; 88:355-365.
- Strasser A. Life and death during lymphocyte development and function: evidence for two distinct killing mechanisms. *Curr Opin Immunol*. 1995;7: 228-234.
- Russell JH. Activation-induced death of mature T cells in the regulation of immune responses. *Curr Opin Immunol*. 1995;7:382-388.
- Mountz JD, Zhou T, Wu J, et al. Regulation of apoptosis in immune cells. *J Clin Immunol*. 1995; 15:1-16.
- Peters AM, Kohfink B, Martin H, et al. Defective apoptosis due to a point mutation in the death domain of CD95 associated with autoimmune lymphoproliferative syndrome, T-cell lymphoma, and Hodgkin's disease. *Exp Hematol*. 1999;27: 868-874.
- Straus SE, Jaffe ES, Puck JM, et al. The development of lymphomas in families with autoimmune lymphoproliferative syndrome with germline Fas mutations and defective lymphocyte apoptosis. *Blood*. 2001;98:194-200.
- Fisher GH, Rosenberg FJ, Straus SE, et al. Dominant interfering Fas gene mutations impair apoptosis in a human autoimmune lymphoproliferative syndrome. *Cell*. 1995;81:935-946.
- Jackson CE, Fischer RE, Hsu AP, et al. Autoimmune lymphoproliferative syndrome with defective Fas: genotype influences penetrance. *Am J Hum Genet*. 1999;64:1002-1014.
- Wang J, Zheng L, Lobito A, et al. Inherited human caspase 10 mutations underlie defective lymphocyte and dendritic cell apoptosis in autoimmune lymphoproliferative syndrome type II. *Cell*. 1999; 98:47-58.
- Ramenghi U, Bonissoni S, Migliaretti G, et al. Deficiency of the Fas apoptosis pathway without Fas gene mutations is a familial trait predisposing to development of autoimmune diseases and cancer. *Blood*. 2000;95:3176-3182.
- Canale VC, Smith CH. Chronic lymphadenopathy simulating malignant lymphoma. *J Pediatr*. 1967; 70:891-899.
- Drappa J, Vaishnav AK, Sullivan KE, Chu JL, Elkon KB. Fas gene mutations in the Canale-Smith syndrome, an inherited lymphoproliferative disorder associated with autoimmunity. *N Engl J Med*. 1996;335:1643-1649.
- Bleesing JJ, Brown MR, Straus SE, et al. Immunophenotypic profiles in families with autoimmune lymphoproliferative syndrome. *Blood*. 2001;98:2466-2473.
- Bettinardi A, Brugnoni D, Quiros-Roldan E, et al. Missense mutations in the Fas gene resulting in autoimmune lymphoproliferative syndrome: a molecular and immunological analysis. *Blood*. 1997; 89:902-909.
- Sneller MC, Straus SE, Jaffe ES, et al. A novel lymphoproliferative/autoimmune syndrome resembling murine lpr/gld disease. *J Clin Invest*. 1992;90:334-341.
- Rieux-Laucat F, Le Deist F, Hivroz C, et al. Mutations in Fas associated with human lymphoproliferative syndrome and autoimmunity. *Science*. 1995;268:1347-1349.
- Sneller MC, Wang J, Dale JK, et al. Clinical, immunologic, and genetic features of an autoimmune lymphoproliferative syndrome associated with abnormal lymphocyte apoptosis. *Blood*. 1997;89:1341-1348.
- Le Deist F, Emile JF, Rieux-Laucat F, et al. Clinical, immunological, and pathological consequences of Fas-deficient conditions. *Lancet*. 1996;348:719-723.
- Infante AJ, Britton HA, DeNapoli T, et al. The clinical spectrum in a large kindred with autoimmune lymphoproliferative syndrome caused by a Fas mutation that impairs lymphocyte apoptosis. *J Pediatr*. 1998;133:629-633.
- Wu J, Wilson J, He J, et al. Fas ligand mutation in a patient with systemic lupus erythematosus and lymphoproliferative disease. *J Clin Invest*. 1996; 98:1107-1113.
- Holzelova E, Vonarbourg C, Stolzenberg MC, et al. Autoimmune lymphoproliferative syndrome with somatic Fas mutations. *N Engl J Med*. 2004; 351:1409-1418.
- Vaishnav AK, Orlicki JR, Chu JL, et al. The molecular basis for apoptotic defects in patients with CD95 (Fas/Apo-1) mutations. *J Clin Invest*. 1999; 103:355-363.
- Boise LH, Gonzalez-Garcia M, Postema CE, et al. bcl-x, a bcl-2-related gene that functions as a dominant regulator of apoptotic cell death. *Cell*. 1993;74:597-608.
- Wang L, Miura M, Bergeron L, Zhu H, Yuan J. lch-1, an lce/ced-3-related gene, encodes both positive and negative regulators of programmed cell death. *Cell*. 1994;78:739-750.
- Alnemri ES, Fernandes-Alnemri T, Litwack G. Cloning and expression of four novel isoforms of human interleukin-1 beta converting enzyme with different apoptotic activities. *J Biol Chem*. 1995; 270:4312-4317.
- Shaham S, Horvitz HR. An alternatively spliced *C. elegans ced-4* RNA encodes a novel cell death inhibitor. *Cell*. 1996;86:201-208.
- Jiang ZH, Zhang WJ, Rao Y, Wu JY. Regulation of lch-1 pre-mRNA alternative splicing and apoptosis by mammalian splicing factors. *Proc Natl Acad Sci U S A*. 1998;95:9155-9160.
- Jiang ZH, Wu JY. Alternative splicing and programmed cell death. *Proc Soc Exp Biol Med*. 1999;220:64-72.
- Liu C, Cheng J, Mountz JD. Differential expression of human Fas mRNA species upon peripheral blood mononuclear cell activation. *Biochem J*. 1995;310(pt 3):957-963.
- Cascino I, Ficuci G, Papoff G, Ruberti G. Three functional soluble forms of the human apoptosis-inducing Fas molecule are produced by alternative splicing. *J Immunol*. 1995;154:2706-2713.
- Papoff G, Cascino I, Eramo A, et al. An N-terminal domain shared by Fas/Apo-1 (CD95) soluble variants prevents cell death in vitro. *J Immunol*. 1996; 156:4622-4630.
- Cheng J, Zhou T, Liu C, et al. Protection from Fas-mediated apoptosis by a soluble form of the Fas molecule. *Science*. 1994;263:1759-1762.
- Forch P, Puig O, Kedersha N, et al. The apoptosis-promoting factor TIA-1 is a regulator of alternative pre-mRNA splicing. *Mol Cell*. 2000;6:1089-1098.
- Cascino I, Papoff G, Eramo A, Ruberti G. Soluble Fas/Apo-1 splicing variants and apoptosis. *Front Biosci*. 1996;1:d12-d18.
- Roesler J, Brenner S, Bukovsky AA, et al. Third-generation, self-inactivating gp91(phox) lentivector corrects the oxidase defect in NOD/SCID mouse-repopulating peripheral blood-mobilized CD34⁺ cells from patients with X-linked chronic granulomatous disease. *Blood*. 2002;100:4381-4390.
- Malech HL, Maples PB, Whiting-Theobald N, et al. Prolonged production of NADPH oxidase-corrected granulocytes after gene therapy of chronic granulomatous disease. *Proc Natl Acad Sci U S A*. 1997;94:12133-12138.
- Kang SM, Braat D, Schneider DB, et al. A non-cleavable mutant of Fas ligand does not prevent neutrophilic destruction of islet transplants. *Transplantation*. 2000;69:1813-1817.
- Martin DA, Zheng L, Siegel RM, et al. Defective CD95/APO-1/Fas signal complex formation in the human autoimmune lymphoproliferative syndrome, type Ia. *Proc Natl Acad Sci U S A*. 1999; 96:4552-4557.
- Siegel RM, Frederiksen JK, Zacharias DA, et al. Fas preassociation required for apoptosis signaling and dominant inhibition by pathogenic mutations. *Science*. 2000;288:2354-2357.
- Wood CM, Goodman PA, Vassilev AO, Uckun FM. CD95 (APO-1/FAS) deficiency in infant acute lymphoblastic leukemia: detection of novel soluble Fas splice variants. *Eur J Haematol*. 2003;70:156-171.
- Liu JH, Wei S, Lamy T, et al. Blockade of Fas-dependent apoptosis by soluble Fas in LGL leukemia. *Blood*. 2002;100:1449-1453.
- Kamihira S, Yamada Y, Tomonaga M, Sugahara K, Tsuruda K. Discrepant expression of membrane and soluble isoforms of Fas (CD95/APO-1) in adult T-cell leukaemia: soluble Fas isoform is an independent risk factor for prognosis. *Br J Haematol*. 1999;107:851-860.
- Inaba H, Komada Y, Li QS, et al. mRNA expression of variant Fas molecules in acute leukemia cells. *Am J Hematol*. 1999;62:150-158.